**Hydrology and
Earth System
Sciences
Discussions**

Quantification of pore-size spectrums by solute breakthrough curves

S. Erşahin

Department of Forest Engineering, School of Forestry, Çankırı Karatekin University, 18100 Çankırı, Turkey

Correspondence to: S. Erşahin (ersahin@karatekin.edu.tr)

HESSD

8, 8373–8397, 2011

Quantification of pore-size spectrums by solute breakthrough curves

S. Erşahin

Title Page

Abstract | Introduction

Conclusions | References

Tables | Figures

◄ | ►►

◄ | ►

Back | Close

Full Screen / Esc

Printer-friendly Version

Interactive Discussion

Abstract

Breakthrough of conservative tracers may be used to quantify pore-size spectrum and pore-water velocity distributions in a porous medium. In this study, a theory was proposed to calculate pore-water velocity and corresponding pore-size spectrum in porous media, and its application was demonstrated. Miscible displacement tests of chloride were conducted with sand columns (5 cm id and 5 cm length), repacked with washed sand with a particle size of 2–1, 1–0.45, 0.45–0.325 and <0.325 mm in diameter. The resulting breakthrough curves were divided into approximately 20 segments, and for each segment, a concentration of Cl in an out-flowing effluent was used with corresponding effluent volume and travel time to calculate corresponding pore water velocity (v) and pore-radius. Mean v (v_b) calculated for a column was approximated by geometric averaging the calculated v-values for the BTC. To validate the developed model, laboratory measured and approximated values of v_b were compared. The correlation analysis conducted between measured and approximated v_b resulted in a correlation coefficient of $r = 0.89$ ($P < 0.01$). The results revealed that size distribution of effective pores could be quite different even in replicates of small sand columns, which are highly similar in particle-size and total porosity.

1 Introduction

Quantitative description of effective pore-size spectrum in soils is challenging work due to complex nature of pore-geometry. As reported by Bouma (1991) and Deeks et al. (1999), several methods have been developed and studied to quantitatively analyze pore characteristics in soils and similar porous media. Methods such as computerized classification and recognition, image analysis, and digital binary images provide a 2-D interpretation of soil morphology. A serial sectioning technique can provide a 3-D interpretation of soil pore space morphology, however, this method requires sophisticated equipment that is not readily available and is also time consuming to perform (Deeks

et al., 1999). Water desorption and mercury intrusion methods are also used widely to determine spectrum of soil pore-size. Since water desoprtion methods are generally conducted on small destructed soil samples, this method addresses only the matrix pore-size spectrum (Kung et al., 2005). In addition, as soil is dried and then liquid

5 is forced into it under pressure, a mercury intrusion method may overestimate the effective pore radii (Radulovich et al., 1989). The details on the principles of these and other methods can be found elsewhere (Bouma, 1991; Lal and Shukla, 2004). Besides the aforementioned methods of soil pore spectrum analysis, water (Radulovich et al., 1989) and solute breakthrough curves (Deeks et al., 1999, 2008; Kung et al., 2000,

10 2005, 2006) were utilized to analyze effective pore-size spectrum and corresponding water flux distribution in soils.

Assessment of pore-size distribution is a major target in the evaluation of water, solute, and air transport in soils (Lal and Shukla, 2004). Kung et al. (2006) stressed that quantitative methodologies for evaluating effective pore-size spectrum are urgently

15 needed.

Radulovich et al. (1989) conducted a water breakthrough study, an extension of a concept of the solute breakthrough curves developed by Nielsen and Biggar (1961), to characterize pore-size spectrum and corresponding water flow characteristics of soil macropores in a well-aggregated Oxic Dystropept. They measured water breakthrough

20 outflow on undisturbed soil cores from a drained state to a saturated state, and calculated macropore-size and -frequency by travel time and the amount of water collected at consecutive steps. They calculated the micropore-size specrum with a pressure plate apparatus, and then they combined macropore-size and micropore-size spectrums to obtain an entire pore-size spectrum of the soils. Kung et al. (2005) used solute break-

25 through curves to analyze pore-size distribution in two intact isolated blocks from a grassland, using the functional relationship between time needed for a tracer to travel a known length of the soil block and radii of the pores through which displacing solution flows with a known velocity. Deeks et al. (1999) related observed changes in solute concentration following a miscible displacement of a $250\,\mathrm{mg\,l^{-1}}$ Cl solution to

characterize size-distribution of large soil conduits. In that study, they calculated volume of discharging traced fluid in a specified time together with the observed rate of movement of tracer within the soils to calculate pore-radius by Poiseuille's equation. Later, Deeks et al. (2008) characterized flow paths and saturated conductivity distribution in 2.4–x 3.4–x 1–m lysimeters. They applied the tracer onto the soil surface and collected soil solution in different locations of the lysimeters, and then they classified the breakthrough curves into statistically distinct pathway types. Kung et al. (2005) proposed field trace mass flux breakthrough patterns to quantify equivalent pore-size spectrum. They used an improved tile drain monitoring protocol, applying a tracer to a narrow strip to a tile-line to measure breakthrough pattern of a tracer mass flux, and used the measured breakthrough curves as surrogates to drive pore spectrum of preferential pathways.

Many miscible displacement studies have shown that one of the most important physical features of the porous media was a magnitude of the volume of water not readily displaced, often termed as immobile or less mobile water. In this study, it was hypothesized that the volume and tracer concentration of discharging traced fluid in a miscible displacement of a conservative tracer can be used to calculate pore-size spectrum. The objectives of this study were (i) to develop a procedure to utilize breakthrough curves of conservative tracers to calculate effective pore-size spectrum for entire range of effective pore-size and (ii) to calculate corresponding pore water velocity spectrum in a porous medium. The theory and principles developed were applied to data of BTCs of chloride from five-cm long and five-cm wide sand columns repacked with different-sized homogenous sand. These small columns were preferred to keep the media as uniform as possible and different-sized homogenous sand was repacked to evaluate model's response to gradually decreased particle-size.

2   Theory and calculations

Hydrodynamic dispersion and convection are the main processes controlling the transport of a conservative tracer (i.e. chloride) in soils and similar porous media (i.e. columns of glass beads). In a miscible displacement, volume of displacing effluent (ΔQ), needed to transport a known amount of the conservative tracer by convective flow (assuming no lateral mass exchange and hydrodynamic dispersion for now) from the inlet to outlet of a column may be calculated as follows:

$$\Delta Q = \frac{\Delta M \Delta V}{M} \tag{1}$$

where, M is the concentration (in molar) of tracer at the inlet of the column (stock solution), ΔM is the difference in the concentration of the tracer at the outlet between times t_i and t_{i+1}, and ΔV is the volume of effluent collected between t_i and t_{i+1}.

Applied to the BTC, Eq. (2) results in:

$$\Delta Q = \Delta \left(C/C_0\right) \Delta \left(P/P_0\right) P_0 \tag{2}$$

where, $\Delta \left(C/C_0\right)$ is the difference in dimensionless concentration (it is equal to $\Delta M/M$ in Eq. 1), $\Delta \left(P/P_0\right)$ is difference in dimensionless pore volume, and P_0 (L^3) is the pore volume of porous media (amount of effluent held in the column). The property $\Delta \left(P/P_0\right)P_0$ is equal to ΔV in Eq. (1). It is assumed that the porous system is made up bundles of different sized capillaries. Each size-class (bundle) has a mean equivalent diameter, which controls the rate of effluent flow and transport characteristics. The Eq. (2) assumes intrinsically that original solute entering the capillaries arrives in the outlet of the capillaries; that is no solutes are lost or gained by lateral diffusive mass exchange and/or no solutes are transported by hydrodynamic dispersion. This means that, the Eq. (2) simply applies to a *piston flow*. However, the piston flow never occurs in practice, as lateral mass exchange between effluent in the effective capillaries and in matrix capillaries (pores) takes place, and part of the solute is transported by hydrodynamic

dispersion. Therefore, the combined effect of lateral mass exchange and hydrodynamic dispersion results in a "dilution of original solution (solution applied from the inlet of the column or simply stock solution)" during the transport in the capillary. In a piston flow, when the dimensionless pore number is one ($P/P_0 = 1.0$), relative solute concentration at the outlet of the column is unity ($C/C_0 = 1.0$), meaning that all the effective capillaries in the system are saturated by displacing solution. Thus, to account for lateral mass exchange and hydrodynamic dispersion effect, the right hand side of Eq. (2) may be multiplied by $P/P_{0(C/C_0=1.0)}$ where all the effective capillaries are saturated by displacing effluent. This results in Eq. (3):

$$\Delta Q_a = \Delta\left(C/C_0\right)\left(P/P_0\right)\left(P/P_0\right)_{(c/c_0=1.0)} \tag{3}$$

where $(P/P_0)_{(C/C0=1.0)}$ is (P/P_0) at $C/C_0 = 1.0$ and ΔQ_a is the hydrodynamic dispersion-adjusted value of ΔQ. Derivation of adjustment factor $(P/P_0)_{(C/C0=1.0)})$ will be discussed in more detail in Sect. 5.

Mean pore-water velocity v_i (LT^{-1}) for a capillary class i can be calculated by:

$$v_i = \frac{\tau l}{t_{ci}} \tag{4}$$

where, τ is mean tourtuousity of the pores (–), l is the length of the column (cm), and t_{ci} is the cumulative of the time (s) elapsed from the moment at which displacing effluent is first applied to the column. The value for τ was assumed as 1.1 for small columns repacked with well-sorted sands, the lowest value for soils (Radulavich et al., 1989). Radii of capillaries in a size-class can be calculated by (Jury et al., 1991);

$$r_i = (v_i\, \tau l\, \gamma)^{1/2} \tag{5}$$

where, γ is the kinematic viscosity for water (10^{-4} cm s^{-1}) (Freeze and Cherry, 1979). If volume flow rate per unit area is known, number of pores (n_i) with equivalent radius in a size-class (r_i) can be calculated by Eq. (6) (Jury et al., 1991):

$$n_i = \frac{Q_i}{\pi\, r_i^{1/2}}, \tag{6}$$

where,

$$Q_i = \frac{\Delta Q_{i\mathrm{a}}}{t_{i+1} - t_i}. \tag{7}$$

In Eq. (7), $t_{i+1} - t_i$ is the time elapsed (s), during which volume of traced effluent is collected to calculate $\Delta Q_{i\mathrm{a}}$ (see Eq. 3).

The average value of pore water velocity (v_b) for all the effective capillaries in the column can be calculated by taking geometric mean of values calculated for all the capillary bundles (size-classes corresponding to segments of BTC) corresponding to entire range of BTC. Therefore, v_b of the column can be approximated by:

$$v_\mathrm{b} = (v_1 + \ldots + v_n)^{1/n} \tag{8}$$

where v_1 is the v_i corresponding to the first segment and v_n is the v_i corresponding to the last segment of the breakthrough curve.

Total amount of mobile water in the column can be calculates as:

$$Q_\mathrm{m} = \sum_{i=1}^{n} Q_{i\mathrm{a}}. \tag{9}$$

Finally, mobile water fractionation coefficient, β, can be calculated by Eq. (10):

$$\beta = P_0 / Q_\mathrm{m} \tag{10}$$

where, P_0 is the amount of water held in the column (pore volume; cm^3) during the test.

3 Experimental

3.1 Materials and methods

The theory and methodology proposed in Sect. 2 were applied to experimental break-through curves (BTCs) of chloride, obtained on small sand columns (5 cm length and 5 cm id) repacked with washed sand.

Triplicate sand columns were repacked with sand, screened through 2, 1, 0.425 and 0.325 mm openings. To achieve a uniform packing, the bottoms of the columns were gently tapped on the laboratory bench 20 times during packing.

3.1.1 Miscible displacement tests

Before conducting a miscible displacement test, both ends of the soil column were supported with a fabric. The column then was gradually saturated with a 0.01 M KBr solution from the bottom (van Genuchten and Wierenga, 1977). Upon saturation, the column was positioned on an upright stand. The inlet at the top of the column was connected to a mini-disc infiltrometer with a bottom of 5 cm diameter that just fitted to the top of the column with 5 cm of id. After steady state flow was established under zero tension, approximately 6.0 pore volumes of tracer solution of 0.05 CaCl$_2$ in 0.01 M KBr solution was introduced into the column with the disc infiltrometer under zero tension. The effluent was collected manually, and analyzed for chloride by the potentiometric titration method (Adriano and Doner, 1982)

Following the miscible displacement tests, the column was taken out and placed in an oven with a constant temperature of 105 °C to measure bulk density and calculate total porosity f. The total porosity was calculated by;

$$f = 1 - \frac{D_b}{D_p} \tag{11}$$

where D_b is bulk density (ML^{-3}) of the column and D_p is the density of particles (ML^{-3}), assumed as $2.65\,Mg\,m^{-3}$. The saturated water content of the column was deemed equal to the volume of pores in sand column.

Dimensionless concentrations of chloride were calculated, dividing the concentration of chloride in the effluent measured by potentiometric titration method to the concentration in the stock solution measured by the same method.

3.1.2 Calculation of v, r, and n for capillary classes (bundles)

Each breakthrough curve was divided into approximately 20 segments, the first segment being with the smallest $C/C_0 > 0$ and the last one with greatest C/C_0. For each segment, v ($cm\,s^{-1}$) was calculated by Eq. (4) using $l = 5.0\,cm$ (length of the column), $\tau = 1.1$ (Radulaviich et al., 1989), and t_i = time elapsed from the moment at which the displacing effluent (Cl) applied to the column. Radius of each capillary class was calculated using the calculated v_i values with Eq. (5), and number pores (n) in each capillary class was calculated using the calculated r_i values and Q_i values with Eq. (6). The values for Q_i was calculated by Eq. (7), dividing the value calculated by Eq. (3) by $t_{i+1} - t_i$, where t_i beginning and t_{i+1} is the ending time for step (segment) i. Finally, a mobile water partitioning coefficient β was calculated by Eq. (9)

Verification of calculations

Mean pore water velocity of the saturated column (v_b) was calculated using the v-values calculated for all the segments (pore-size classes) with Eq. (8). To verify the modeling results, the measured values of v at saturated column (v_{bm}) were plotted (H-scatterplot) against v_b values calculated by Eq. (8). Coalescence of the data around a 45°-diagonal was interpreted as a qualitative measure of the similarity of measured and calculated values of mean pore water velocity (and also mean saturated hydraulic conductivity). To evaluate the similarity quantitatively, the measured values were correlated to modeled values. The extent of correlation coefficient was considered in assessing

the success of the technique developed. Since it takes a considerably long time to complete a miscible displacement test in unsaturated conditions, the validation was constrained to saturated conditions.

4   Results

The properties of the sand columns used in miscible displacement of chloride are given in Table 1. As expected, lowest bulk density D_b occurred with the smallest particle size. The triplicates were quite similar in D_b, total porosity f, saturated water content θ_s, and pore volume at saturation P_0. Pore water velocity v (cm s^{-1}) decreased gradually versus the decreasing particle-size of the repacked sand.

The breakthrough curves of chloride and corresponding v and pore number (n) in each capillary size class are presented in Figs. 1–4. In general, the BTCs gradually shifted to right with decreasing particle-size as indicated by trajectories of BTCs at P/P_0 against $C/C_0 = 0.5$. Nielsen and Biggar (1961) attributed the right-shift in their study to amount of water not displaced during the miscible displacement. Figures 1–4 show that considerable amount water was not displaced in the columns and that calculated values of mobile water fraction (β) in the columns were not correlated to particle-size. Angulo-Jaramillo et al. (1996) measured mobile water content with a disc infiltrometer, adding a Cl tracer after pre-wetting the soil with water. Their results showed that the mobile water content was a function of mean pore-size, described by an s-shaped curve showing the continuous change in the mobile water content ratio from the microporus to the macroporus system. That β in this study was not related to particle-size may be attributed to the difference in calculation of β between this study and study by Angulo-Jaramillo et al. (1996).

The variable β represents fraction of mobile water – mobile water/(mobile water plus immobile or less mobile water) – in the column. The parameter β is somehow similar in 2-mm size replicates, ranging from 0.18 to 0.24 (Fig. 1). However, for the same

replicates, the effective pore-size spectrum differs considerably in both number of pores and range of pore-size. For example, most of the transport was controlled by the pores with radii between 0.01 and 0.006 cm in the first replicate (the upper graph in Fig. 1), however, the transport was controlled by pores of completely different sizes in the third replicate (the bottom graph in Fig. 1). In addition, the peak location and height shift of n considerably differs in replicates given in Figs. 1–4.

Similar conclusions can be made for other tests conducted with lower particle sizes. For example, Fig. 2 shows that the third replicate has a highly different pore-size spectrum than other two replicates. In addition, although the breakthrough curves of the first and the second replicates are relatively similar; their corresponding pore-size spectrum differs considerably. Second and third replicates in 0.424 mm treatment (Fig. 3) are highly similar in β, however, pore size distribution and v distribution are quite dissimilar. In 0.325 mm treatment (Fig. 4), although first and second replicates resembled in β, their corresponding pore spectrums were exceedingly different.

Mean pore water velocity on saturated columns (v_b) was calculated by Eq. (8), taking geometric average of the v-values calculated for the capillary size classes corresponding to segments of BTCs. The calculated results were compared with measured saturated v-values (v_{bm}) of the columns. In general, the model under predicted mean pore water velocity particularly for greater v_{bm} values (Fig. 5) (those values for 2–1 and 1–0.5 mm sand sizes). However, in overall, the measured and predicted v_b values were highly associated as indicated by high correlation coefficient ($r = 0.89$, $P < 0.01$) calculated between measured and predicted values.

5 Discussion

Hydraulic conductivity can be viewed as contributions from all individual pathways to be lumped into a single value (Kung et al., 2005, 2006). However, this lumped variable may be inadequate when matrix flow is not dominant (Gish et al., 2004). Kung et al. (1995)

stressed that it is intrinsically wrong to use a lumped hydraulic conductivity value to predict convective contaminant transport through preferential flow pathways. Results of this study highly agreed to their conclusions. The lumped hydraulic conductivity value measured for the first replicate of 2–1 mm size class treatment was 0.044 cm s^{-1}. However, the Fig. 1 shows that conductivity of water saturated domains ranges from 0.026 to 0.124 cm s^{-1} and that tremendous of flux is controlled by pores corresponding to water flux rate greater than 0.044 cm s^{-1}, suggesting that use of a single lumped parameter may lead erroneous conclusions as suggested by Kung et al. (2000, 2005, and 2006). Similar conclusions can be made from the other graphs in Figs. 1–4.

In our calculations, the measured K_s for the 2–1 mm size treatment were 0.044, 0.046, and 0.043 for replications 1, 2, and 3, respectively. By these values, it may be concluded that the three replicates are highly similar in K_s. However, Fig. 1 shows tremendous differences in range, number, and distribution of pores in these replicates. In the first replicate, the transport is mainly controlled by pores with radii between 0.008 and 0.006 cm (Fig. 1 top graph), while in second and especially in third replicate, completely different pore-sizes controlled the water and chemical fluxes. Similarly, for the $r < 0.325$ mm particle-size treatment (Fig. 4), the water and solute flux was controlled completely different pore-sizes despite their highly similar K_s values. These pore-spectrums, measured in highly homogenized conditions (small columns repacked with sieved washed sands) were considerably different. In structured media, far more differences are expected, and these show that a single lumped parameter is inadequate to represent all these differences in pore characteristics that ultimately have an important impact on water and chemical fluxes in soils.

Shape of BTCs is generally interpreted to qualitatively assess physical and chemical characteristics of transmitting media. The method developed in this study made this interpretation more fruitful, translating the details in a BTC to better interpretable pore-size spectrum and corresponding pore-water velocity distribution information. For example, in Fig. 3, it is highly difficult to compare the BTCs of the second and third replicates in terms of pore-size spectrum and pore water velocity distributions without

Full Screen / Esc

Printer-friendly Version

Interactive Discussion

graphs given in middle and right columns since two graphs are similar. However, the pore-size distribution and corresponding pore-water velocity distribution graphs reveal many details in pore characteristics.

The capacity of the soils to store and transmit water and nutrients is hinged on the porous nature of the soils (Kung et al., 2005). Attempts have been made to better represent the pore characterisitics in flow domains in water and solute transport studies. The two-domain approach (van Genuchten and Wierenga, 1976) and multiple domain approach (Gwo et al., 1995) were proposed to compensate the drawback form use of a single lumped variable, mean hydraulic conductivity (Kung et al., 2005). Durner and Fluhler (1996) suggested that a continuous pore spectrum is necessary to simulate chemical transport and proposed that multiple domain approach should be used as an alternative to the lumped parameter, hydraulic conductivity. The stream tube model from Toride et al. (1995) was fundementally similar to multiple domain approach. The stream tube model assumes that the each stream tube can be treated theoretically as an independent domain. The multiple domain approach is highly daunting in measuring hydraulic conductivity for a soil that is divided further into more domains. Also, defining the boundaries among domains and tubes is very difficult and the success of using multiple domains depends firmly on the accurate measurement of hydraulic conductivity of these domains (Kung et al., 2005). The procedure developed in this study allows us to divide the system with as many domains (segments) as desired and to define boundaries among domains.

Methodlogy, partly similar to one developed in this study, was used by others (Kung et al., 2005) to quantify the spectrum of macropore-type preferential pathways using BTCs of conservative tracers. They used an improved tile drain monitoring protocol and they applied tracers to a narrow strip near the tile line and measured breakthrough patterns of tracer mass flux. They used BTCs as surrogates to find the parameters of the proposed function to derive the pore-spectrum of preferential pathways. However, their model did not account for hydrodynamic dispersion and chemical adsorption effects. In a similar fashion, Deeks et al. (2008) characterized flow paths and saturated

Title Page

Abstract | Introduction

Conclusions | References

Tables | Figures

◄◄ | ►►

◄ | ►

Back | Close

Full Screen / Esc

Printer-friendly Version

Interactive Discussion

conductivity in a large soil block in relation to chloride BTCs. In another study, Deeks et al. (1999) found that solute movement was predominantly confined to pores with radii between 0.3 and 1.0 mm. The method developed by Radulovich et al. (1989) predicts pore-size spectrum as combination of water breakthrough curves and moisture release curves. However, use of the moisture release curves is criticized since these curves are typically measured using homogenized soils where the soil structural pores were destroyed.

The model developed in this study can be used to measure the size spectrum of all hydraulically active pores in a porous medium. The model accounts for hydrodynamic dispersion as well as lateral mass exchange between mobile domains and between mobile and stagnant (or less mobile) domains. The following mental experiment leads us to intrinsically introduce an "adjustment factor ($P/P_{0(C/C0=1.0)}$)" used in (Eq. 3) to account for effect of hydrodynamic dispersion and lateral mass exchange: In "piston flow" (Fig. 6), whole pores in the system are in same radius and saturated by the traced effluent where $P/P_0 = 1.0$. The entire effluent in the system contributes transport and, therefore, there is no immobile water in the column. Furthermore, all the chemical is transported by convective flow and no hydrodynamic dispersion presents in the system as indicated by $P/P_0 = 1.0$ against $C/C_0 = 1.0$. Therefore, the conditions for the piston flow may be used as a reference point ($P/P_0 = 1.0$ against $C/C_0 = 1.0$) to account for "dilution effect" caused by hydrodynamic dispersion and lateral exchange between mobile/less mobile and immobile regions. Any discrepancy (early appearance and delay) from this reference point can be accounted as effect of hydrodynamic dispersion and lateral solute exchange among the flow domains. Therefore, as an account of hydrodynamic dispersion, the BTC diverse from the piston flow, taking different values of P/P_0 against C/C_0 as a response to dilution effect caused by hydrodynamic dispersion and interactions among flow domains. Apart from this, we may multiply the Eq. (2) by $P/P_{0(C/C0=1.0)}$ as an adjustment factor, resulting in Eq. (3).

The model developed in this study differs from the those by others in the following aspects. Firstly, the developed model calculates the amount of mobile water for any

desired segment in a BTC. This allows to calculate corresponding number for pores by well known Pouiseille equation, which in turn, leads calculate size spectrum of all effective pores in the system. And secondly, as mentioned above, the model accounts for effects of hydrodynamic dispersion and lateral interactions among domains in a porous system.

The spectrum of hydraulically active pores should be determined to better model water and chemical flux in soils. The pore-size is the key property controlling the convective transport through soils since the flux rate is proportional to the forth power of equivalent pore radius according to well known Poiseuille equation (Jury et al., 1991). In this study, it is assumed that the adjacent flow domains (domains made up similar sized capillary pores) were interacting.

Water flow in soils depends mainly on pore geometry and pore-size distribution, which are controlled by soil structure and soil texture. It is considerably difficult to quantify the relation between soil structure and water and solute transport in soils (Deeks et al., 1999). The theory and applications adapted here suggests there are several directions for future research efforts. Development and application of laboratory techniques for measurement of effective pore-size distribution together with convective flow of water in soils with diverse structure may result in a significant breakthrough in understanding of water and chemical transport in structured soils.

The model developed in this study has several drawbacks. First, it takes quite long time to complete a miscible disparagement test in structured clay soils. In this case, the P/P_0 of the BTC may be extrapolated to $C/C_0 = 1.0$, and this resulting extrapolated value of P/P_0 can be used as an adjustment factor in Eq. (3). Second, in highly structured or macroporous soils, it may be very difficult to catch large macropores, which is very important in preferential transport of water and solutes. This problem can be tackled, conducting a more frequent sampling at the early stage of test. Finally, the BTC should be an increasing function to make calculations, otherwise one may come up with unreasonable values of v, n, and r. Therefore, the measurement device should be very precise that it can measure slight changes in solute concentrations in consecutive

samples. The same is also true for measuring first concentration breakthrough in very early stage of test where largest pores start to discharge the displacing effluent.

6 Conclusions

A theory was proposed to calculate effective pore-size spectrum by breakthrough curves (BTCs) of conservative tracers in soil and similar porous media. The theory was tested using breakthrough curves of chloride from small columns repacked with clean uniform sand material.

Miscible displacement tests of CL were conducted on sand columns repacked with sieved sands of 1–2, 0.425–1, 0.3.25–0.25 and, <0.325 mm, and the resulting BTCs were used to calculate distributions of pore-water velocity and corresponding pore-size spectrums. The rationale behind use of these small columns was to evaluate model in simplest and uniform conditions to decrease number of uncontrolled variables.

Decreased particle-size resulted in increased pore number, slightly increased water content, and decreased mean pore water velocity. A considerable difference occurred among treatments (particle-sizes) as well as replicates of treatments shown by range and height shift of pore-size spectrums. Replicates similar in water content, mean pore water velocity, bulk density, and mobile water content yielded different pore-size spectrums as shown by range and height shift of graphs. Pore water velocity distribution in the columns showed that use of a lumped parameter of hydraulic conductivity may not be adequate in chemical transport modeling studies. The developed model accounts for hydrodynamic dispersion and lateral mass exchange between mobile and immobile/less mobile domains. Another study is currently underway to evaluate the proposed model on disturbed and undisturbed soil columns (30 cm long and 8.5 cm id) to extend its use to more complicated conditions.

References

Adriano, D. C. and Doner, H. E.: Bromine, Chlorine, and Fluorine, in: Methods of Soil Analysis, Part 2, Chemical and Microbiological Properties, 2nd Edn., ASA No: 9 (Part 2), 449–483, 1982.

Angulo-Jaramillo, P., Gaudet, J.-P., Thony, J.-L., and Vauclin, M.: Measurement of hydraulic properties and mobile water content of a field soil, Soil Sci. Soc. Am. J., 60, 710–715, 1996.

Bouma, J.: Influence of soil macroporosity on environmental quality, Adv. Agron., 46, 1–37, 1991.

Deeks, L. K., Williams, A. G., Dowd, J. F., and Scholefield, D.: Quantification of pore size distribution and the movement of solutes through isolated soil blocks, Geoderma, 90, 65–86, doi:10.1016/S0016-7061(98)00092-5, 1999.

Deeks, L. K., Bengough, A. G., Stutter, M. I., Young, I. M., and Zhang, X. X.: Characterization of flow paths and saturated conductivity in a soil block in relation chloride breakthrough, J. Hydrol., 348, 431–441, doi:10.1016/j.jhydrol.2007.10.025, 2008.

Durner, W. and Flühler, H.: Multi-domain model for pore-size dependent transport of solutes in soils, Geoderma, 70, 281–297, 1991.

Freeze, R. A. and Cherry, J. A.: Groundwater, Prentice-Hall Inc., Englewood, NJ, USA, 1979.

Gwo, J. P., Jardine, P. M., Wilson, G. W., and Yeh, G. T.: A multiple pore region concept to modeling mass transfer in subsurface media, J. Hydrol., 164, 217–237, doi:10.1016/0022-1694(94)02555-P, 1995.

Jury, A. W., Gardner, W. R., and Gardner, W. H.: Soil Physics, 4th Edn., John Willey & Sons, Inc., New York, NY, 1991.

Kung, K.-J. S., Klodviko, E. J., Gish, T. J., Steenhuis, T. S., Bubenzer, G., and Helling, C. S.: Quantifying preferential flow by breakthrough of squentially applied tracers: Silt loam soil, Soil Sci. Soc. Am. J., 64, 1296–1304, 2000.

Kung, K.-J. S., Hanke, M., Helling, C. S., Kladivko, E. J., Gish, T. J., Steenhuis, T. S., and Jaynes, D. B.: Quantifying pore-size spectrum of macropore-type preferential pathways, Soil Sci. Soc. Am. J., 69, 1196–1208, doi:10.2136/sssaj2004.0208, 2005.

Kung, K.-J. S., Klodviko, E. J., Helling, C. S., Gish, T. J., Steenhuis, T. S., and Jaynes, D. B.: Quantifying the pore size spectrum of macropore-type preferential pathways under transient flow, Vadose Zone J., 5, 978–989, doi:10.2136/vzj2006.0003, 2006.

Title Page

Abstract | Introduction

Conclusions | References

Tables | Figures

◄ | ►

◄ | ►

Back | Close

Full Screen / Esc

Printer-friendly Version

Interactive Discussion

Lal, R. and Shukla, M. K.: Principles of Soil Physics, Marcel Dekker, Inc., New York, NY, 2004.

Nielsen, D. R. and Biggar, J. W.: Miscible displacement, I. Experimental information, Soil Sci. Soc. Am. Proc., 25, 1–5, 1961.

Nielsen, D. R. and Biggar, J. W.: Miscible displacement, III. Theoretical considerations, Soil. Sci. Soc. Am. Proc., 26, 216–221, 1962.

Nielsen, D. R. and Biggar, J. W.: Miscible displacement, IV. Mixing in glass beads, Soil. Sci. Soc. Am. Proc., 27, 10–13, 1963.

Radulovich, R., Solorzano, E., and Sollins, P.: Soil macropore size distribuiton from water breakthrough curves, Soil Sci. Soc. Am. J., 53, 556–559, 1989.

Toride, N., Leij, F. J., and van Genuchten, M. H.: The CXTFIT Code for Estimating Transport Parameters from Laboratory or Field Tracer Experiments, Version 2, Research Rep. No: 137, US Salinity Laboratory Agricultural Research Service US Department of Agriculture Riverside, CA, 1995.

van Genuchten, M. Th. and Wierenga, P. J.: Mass transfer in sorbing porous media, II. Experimental evaluation with tritium (^{3}H$_2$0), Soil. Sci. Soc. Am. J., 41, 272–278, 1977.

Quantification of pore-size spectrums by solute breakthrough curves

S. Erşahin

Title Page

Abstract	Introduction
Conclusions	References
Tables	Figures

◀◀   ▶▶

◀   ▶

Back   Close

Full Screen / Esc

Printer-friendly Version

Interactive Discussion

Table 1. Properties of Repacked Sand Columns Used in the Miscible Displacement Tests.

Column ID	PS[1] Mm	D_b^2 gr cm^{-3}	f^3 (–)[7]	v^4 cm s^{-1}	θ_s^5 cm^3 cm^{-3}	P_0^6 cm^3
1a	1.0–2.0	1.65	0.38	0.126	0.38	38.0
1b	1.0–2.0	1.62	0.39	0.170	0.39	39.0
1c	1.0–2.0	1.64	0.39	0.114	0.38	38.0
2a	0.425–1.0	1.62	0.39	0.084	0.39	39.0
2b	0.425–1.0	1.61	0.39	0.099	0.39	39.0
2c	0.425–1.0	1.60	0.39	0.110	0.39	39.0
3a	0.350–0.425	1.56	0.41	0.077	0.41	41.0
3b	0.350–0.425	1.56	0.41	0.089	0.41	41.0
3c	0.350–0.425	1.55	0.41	0.090	0.41	41.0
4a	<0.325	1.57	0.41	0.018	0.41	41.0
4b	<0.325	1.58	0.40	0.017	0.40	40.0
4c	<0.325	1.57	0.40	0.016	0.40	40.0

[1] PS: particle size, [2] D_b: bulk density, [3] f: total porosity, [4] v: pore water velocity, [5] θ_s: volumetric water content at saturation, [6] P_0: pore volume of saturated column, [7] (–): dimensionless.
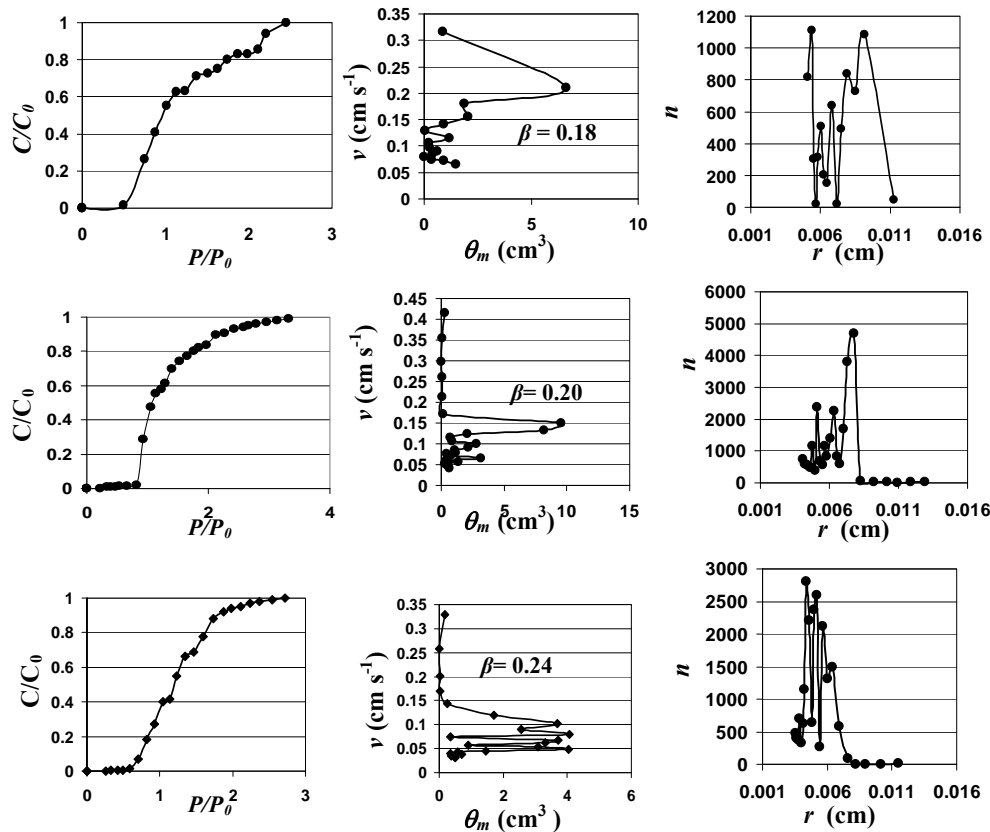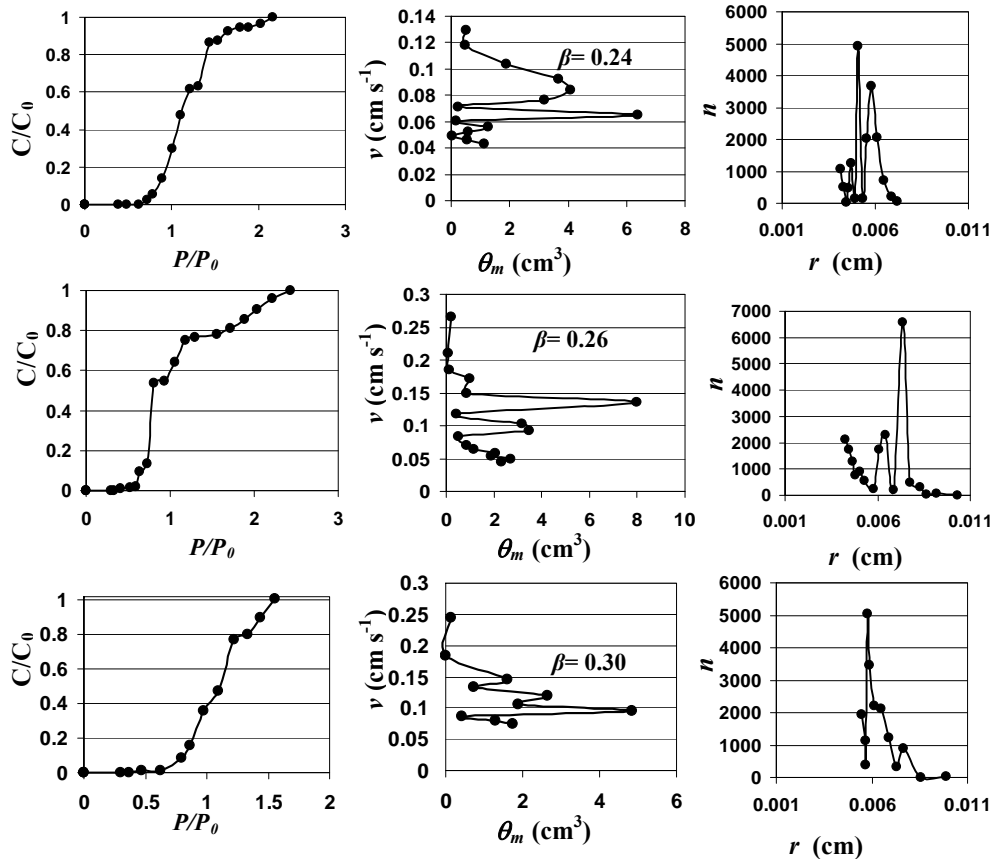
Fig. 1. Breakthrough Curves of Chloride (Left Column), Amount of Mobile Water (θ_{m}) Related to Pore Water Velocity (v) (Middle Column), and Number of Pores (n) Related to Given Pore Radii (r) (Right Column). Miscible Displacement Tests Were Conducted With Columns Repacked With Sand With 1.0–2.0 mm In Diameter. Variable β is Mobile Water Fractionation Coefficient (See Eq. 9 for its Calculation). Top, middle and below lines are replicates.

Title Page

Abstract | Introduction

Conclusions | References

Tables | Figures

◀◀ | ▶▶

◀ | ▶

Back | Close

Full Screen / Esc

Printer-friendly Version
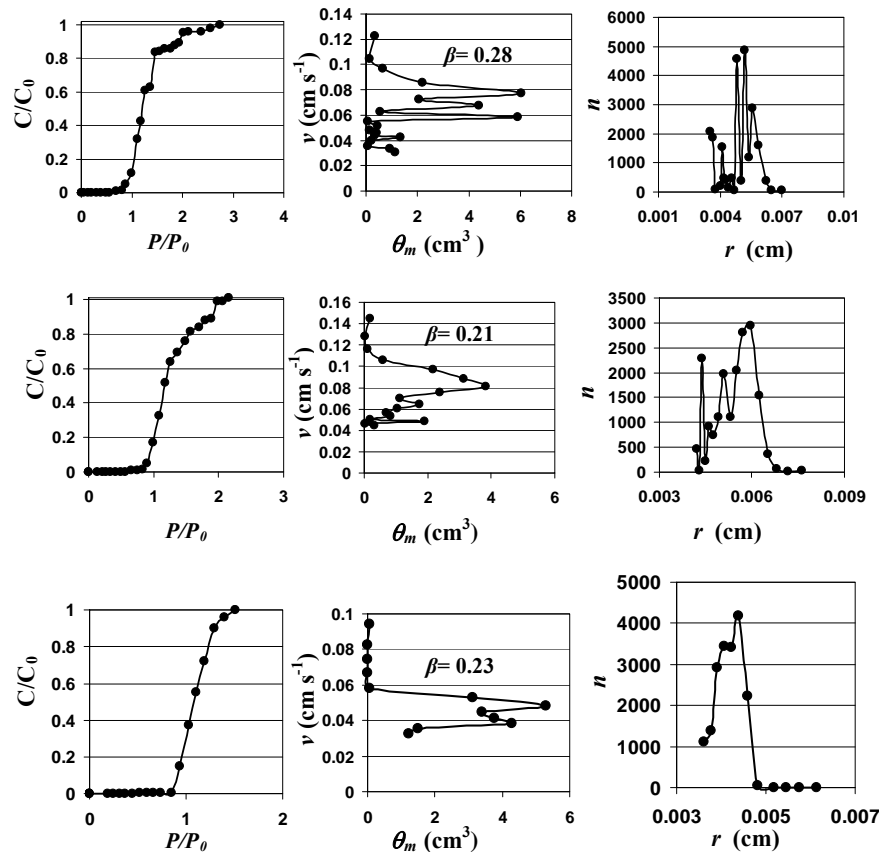
Interactive Discussion

Fig. 2. Breakthrough Curves of Chloride (Left Column), Amount of Mobile Water (θ_m) Related to Pore Water Velocity (v) (Middle Column), and Number of Pores (n) Related to Given Pore Radii (r) (Right Column). Miscible Displacement Tests Were Conducted With Columns Repacked With Sand With 0.5–1.0 mm in Diameter. Variable β is Mobile Water Fractionation Coefficient (See Eq. 9 for its Calculation). Top, middle and below lines are replicates.
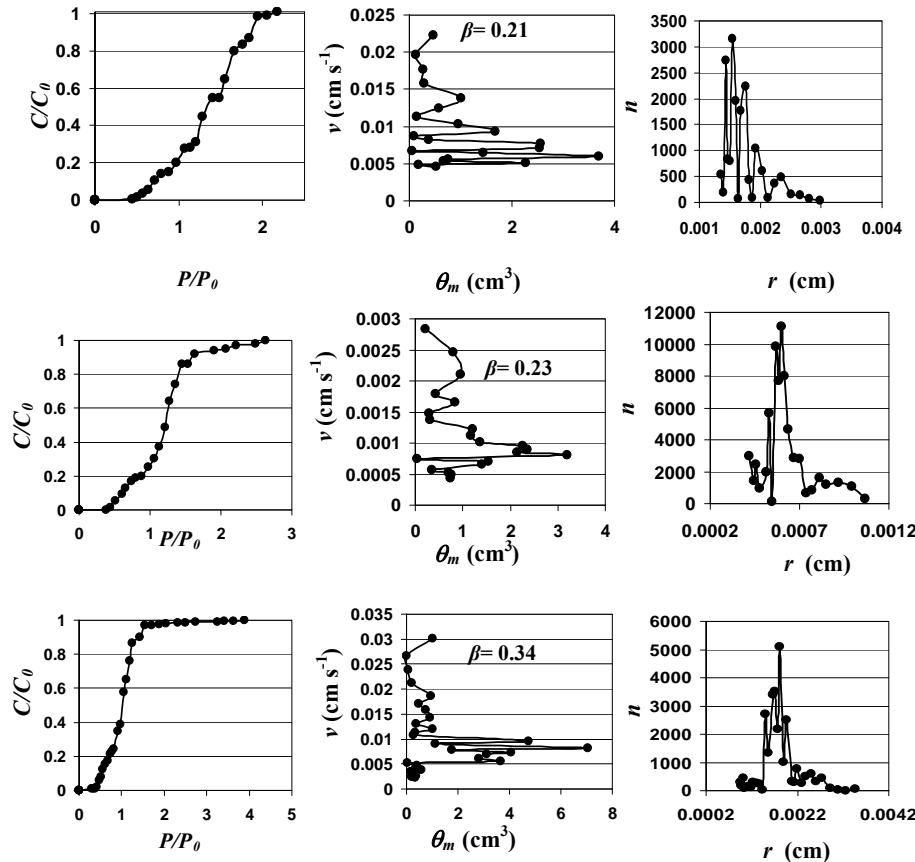
Fig. 3. Breakthrough Curves of Chloride (Left Column), Amount of Mobile Water (θ_m) Related to Pore Water Velocity (v) (Middle Column), and Number of Pores (n) Related to Given Pore Radii (r) (Right Column). Miscible Displacement Tests Were Conducted With Columns Repacked With Sand With 0.425–0.5 mm in Diameter. Variable β is Mobile Water Fractionation Coefficient (See Eq. 9 for its Calculation). Top, middle and below lines are replicates.

Fig. 4. Breakthrough Curves of Chloride (Left Column), Amount of Mobile Water (θ_m) Related to Pore Water Velocity (r) (Middle Column), and Number of Pores (n) Related to Given Pore Radii (r) (Right Column). Miscible Displacement Tests Were Conducted With Columns Repacked With Sand With <0.325 mm in Diameter. Variable β is Mobile Water Fractionation Coefficient (See Eq. 9 for its Calculation). Top, middle and below lines are replicates.

Title Page

Abstract | Introduction

Conclusions | References

Tables | Figures

|◄ | ►|

◄ | ►

Back | Close

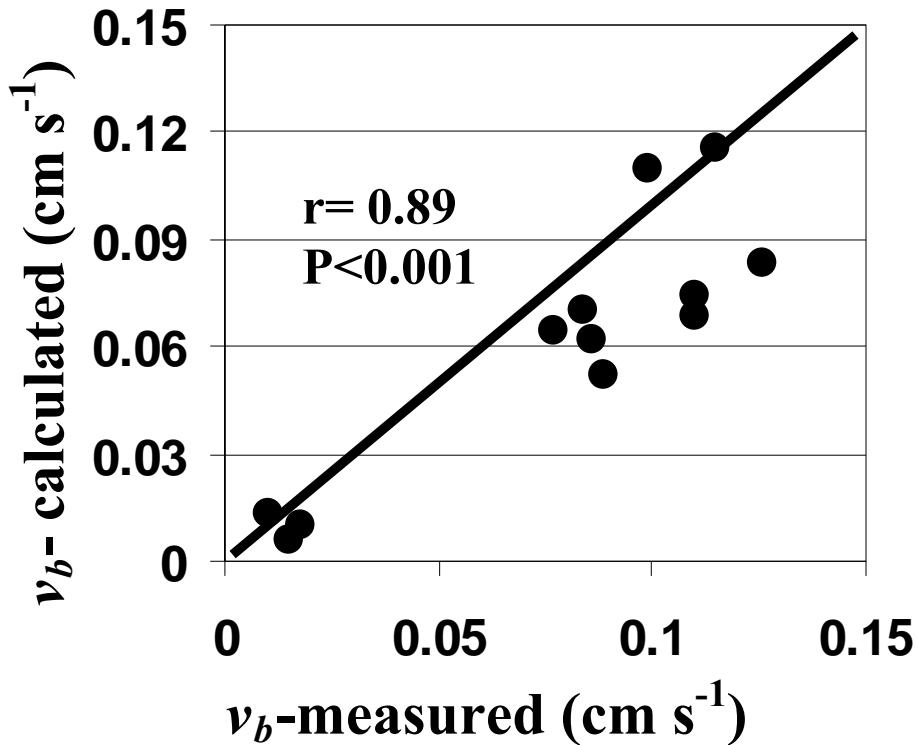Full Screen / Esc

Printer-friendly Version

Interactive Discussion

Fig. 5. Comparison of the Measured and Modeled Values of Mean Pore Water Velocity (v_b). The line is the 45°-diagonal.

The chart shows:
- Y-axis: v_b- calculated (cm s^{-1}), ranging from 0 to 0.15
- X-axis: v_b-measured (cm s^{-1}), ranging from 0 to 0.15
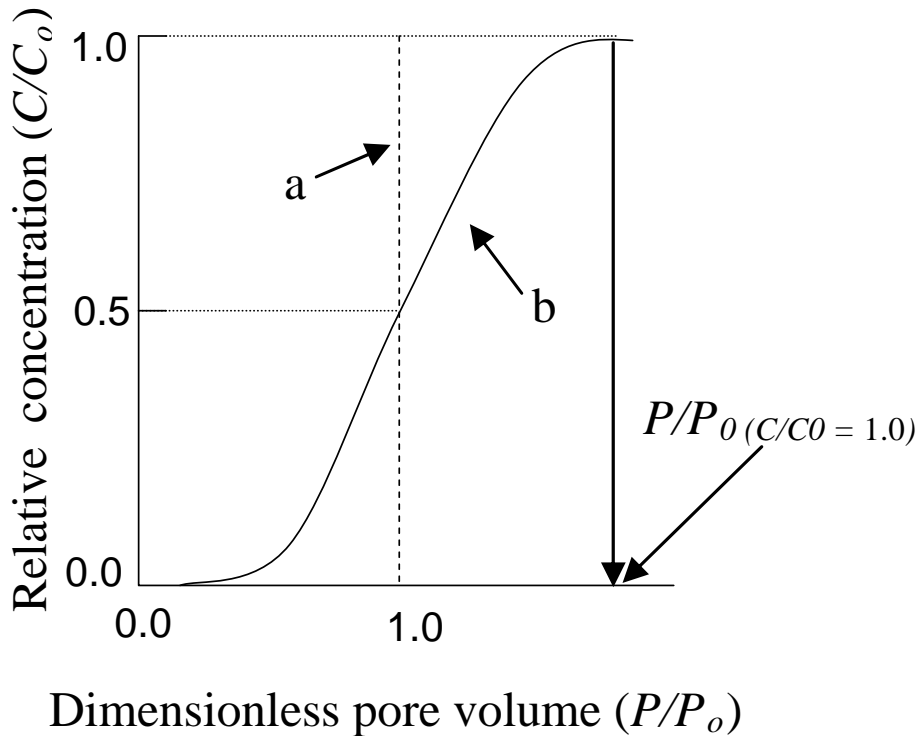- r= 0.89
- P<0.001

Fig. 6. Hypothetical Breakthrough Curves for Different Displacement Conditions **(a)** Piston flow and **(b)** Flow Contributed by Convection, hydrodynamic dispersion, and Lateral mass Exchange between Mobile and Immobile/Less Mobile Regions. The Arrow Shows the Adjustment Factor used with Eq. (3) to Account to Hydrodynamic dispersion and Lateral Mass Exchange Effects. See Text for more Explanation.